Asia-Pacific Conference on FRP in Structures (APFIS 2007)
S.T. Smith (ed)

AN EXPERIMENTAL INVESTIGATION ON THE STRENGTHENING OF RC BEAM-COLUMN CONNECTIONS WITH FRP COMPOSITES

R. Shrestha [1] and S.T. Smith [2]

[1] *Centre for Built Infrastructure Research, The University of Technology Sydney, Australia.*
[2] *Department of Civil Engineering, The University of Hong Kong, China. Email: stsmith@hku.hk*

ABSTRACT

The shear capacity of reinforced concrete (RC) beams-column connections can be enhanced by the addition of externally bonded fibre reinforced polymer (FRP) composites. The FRP can also increase the deformation capacity and energy absorption capacity of the connection. Tests to date have typically involved the application of load in a cyclic push-pull manner and, depending on the design, the connection can fail in various modes ranging from FRP debonding and FRP rupture to failure in the beam, column or joint region. The cyclic nature of the loading however makes it quite difficult to gain a detailed understanding of the behaviour of the FRP alone. In this paper, the results of a detailed experimental study on FRP-strengthened RC beams-column connections with extensive strain gauging of the FRP, internal steel reinforcement and concrete face are reported. The connections were subjected to monotonic loading which allowed the behaviour of the FRP to be closely monitored. The experimental results will serve as a good set of data for future numerical and analytical models to be calibrated against. Finally, experimental results are compared with analytical models.

KEYWORDS

FRP, reinforced concrete, strengthening, beam-column connections, external bonding.

INTRODUCTION

Prior to the implementation of earthquake design standards for the design of reinforced concrete (RC) structures, RC frames were typically gravity load designed. The region where the beam frames into the column, referred to as the *joint*, typically did not require shear reinforcement (also known as *transverse reinforcement*) to be placed (Figure 1). The shear strength of such a joint may therefore not be sufficient to withstand the large induced shear forces generated during a seismic attack. A need therefore exists to not only strengthen existing joints in shear but to also increase their energy absorption capacity.

The use of externally bonded fibre-reinforced polymer (FRP) composites to strengthen shear deficient connections (where *connection* refers to joint region including the beam/s and column/s framing into it) has been proven to be effective (Smith and Shrestha 2006). The majority of research that has been conducted on FRP-strengthened connections to date has however been experimental where both external (i.e. one beam framing into a column) and internal (i.e. two beams framing into a column) two-dimensional connections (Figure 1) have been strengthened in shear with externally bonded FRP. A comprehensive review of experimental research to date in addition to an evaluation of the effectiveness of the strengthening schemes is given in Smith and Shrestha (2006). A review of non-FRP strengthening solutions, as well as some FRP ones, is given in Engindeniz et al. (2005).

The majority of previous experimental studies have reported the behaviour of FRP-strengthened connections subjected to cyclic loading of increasing push-pull amplitude until failure. Hysterisis responses of the connection were typically plotted and the strength, ductility and energy absorption capacity shown to increase. Such tests were therefore aimed at observing the overall behaviour of the connections will limited information on the behaviour of the FRP alone (i.e. such as strain distribution along the FRP strengthening) or detailed reporting of the failure mode.

The primary objectives of the tests reported in this paper were to observe the behaviour of the FRP strengthening and accurately report the failure mode. Extensive instrumentation in the form of linear varying displacement

transducers (LVDTs) and electric strain gauges have been utilised in order to gain an accurate understanding of the behaviour of the various components of the connection. The test connections were also subjected to a monotonically increasing load thus making it easier to observe the behaviour of not only the connection but the FRP strengthening as well. A selection of key results is reported in this paper, namely the results of one control connection as well as two FRP-strengthened connections. Suitable anchorage of the FRP-strengthening was applied in order to prevent premature failure by complete debonding of the FRP.

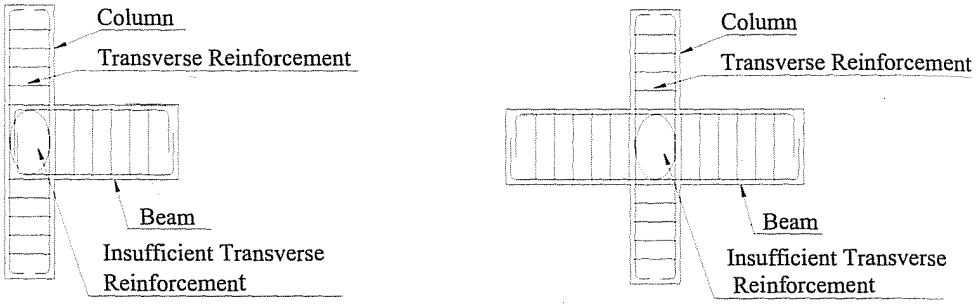

(a) External Connection (b) Internal connection

Figure 1. Connections with shear deficient capacity

EXPERIMENTAL DETAILS

Description of Test Specimens

Three large scale external connections were tested at the University of Technology Sydney's (UTS) structural engineering laboratory facility. One connection was tested as control while the other two were tested after strengthening with FRP. All the connections were designed as being shear deficient by the omission of transverse reinforcement in the joint region as shown in Figure 1a. The geometric properties and reinforcement details of the test connections are shown in Figure 2. The hierarchy of strength design of the connection dictated shear failure in the joint region followed by flexural failure in beam then column failure.

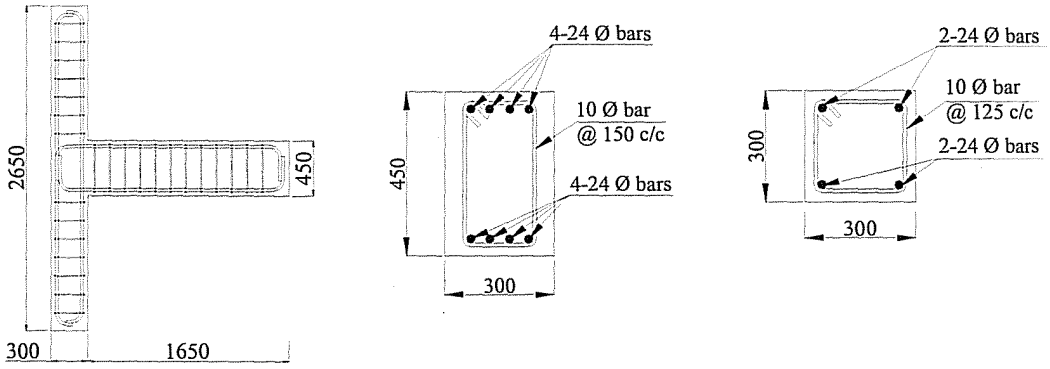

(a) Geometry (b) Beam Section (c) Column Section

Figure 2. Test connection – geometry and reinforcement details

Table 1 presents a summary of the main parameters of the three test connections. Two different FRP-strengthening schemes were employed as shown in Figure 3. The two strengthened connections CF1 and CF2 possessed a common FRP reinforcement ratio ρ_{frp} of 0.052%, where $\rho_{frp} = A_{frp}/bd$, A_{frp} is the cross-sectional area of FRP, b the joint dimension perpendicular to the direction of FRP and d the effective depth of the section (effective depth = distance from the compressive face to the centroid of the internal tension steel of the connection orientation in question). All connections, both control and FRP strengthened were designed to fail in the joint region. The FRP-strengthened connections were designed using theory developed for the shear strengthening design of FRP-strengthened RC beams (Chen and Teng 2003).

All FRP was formed from the wet lay-up procedure and made from carbon sheets of 0.117 mm thickness. The first strengthening scheme (connection CF1, Figure 3a) consisted of two 50 mm wide strips applied on either side of the joint face and extended into the column. Column wraps were provided on both ends of the strip to

provide anchorage against complete debonding as shown in Figure 3a. Two layers of FRP were used in both the strips and in the column wraps. The second strengthening scheme (connection CF2, Figure 3b) consisted of three FRP strips applied parallel to the longitudinal axis of the beam. Each strip was two layers thick and applied around the joint region and extended into the beam in a U-shape. The ends of the strips were anchored using beam wrapping.

The schemes have been chosen keeping in view the need for simplicity and ease in installation in practical applications and are quite fundamental in nature. FRP strips were chosen as opposed to sheets in order to monitor the progression of cracking in the joint region more easily in addition to detecting the occurrence of debonding of the FRP. Also, the beam and column wraps provided anchorage to the FRP strips against global debonding, which makes the strengthening schemes quite unique in nature. In order to ensure good bond between concrete and FRP, the concrete surface was scaled back using a needle gun and all the dust particles were removed with an air gun. Concrete corners were rounded to a radius of 25 mm (ACI440.2R-02 specifies a minimum corner rounding radius of 13 mm).

Table 1. Summary of test connections

Specimen ID	Detail	FRP Orientation	No of strips	Strip Width	Wrap Width
CS1	Control	-	-	-	-
CF1	FRP-strengthened	parallel to column	2	50 mm	300 mm
CF2	FRP-strengthened	parallel to beam	3	50 mm	300 mm

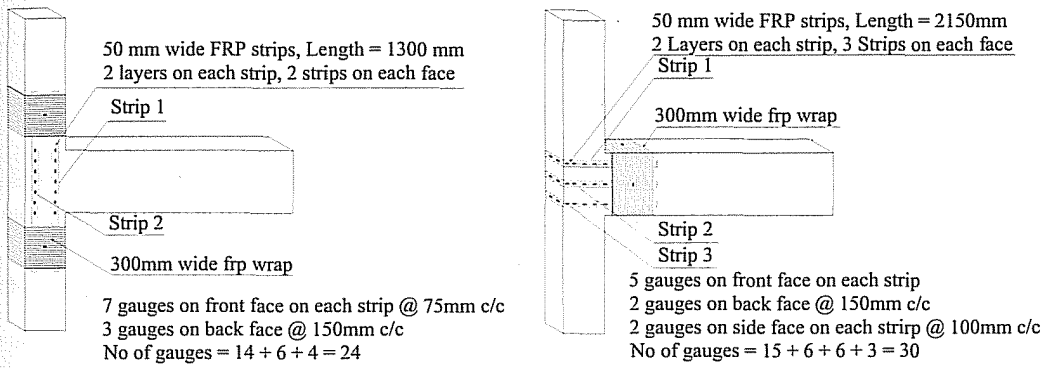

(a) Connection CF1 (b) Connection CF2

Figure 3. FRP strengthening scheme and summary of FRP strain gauges

Material properties

Properties of concrete on the day of the corresponding connection test are given in Table 2. As the concrete was a few months old, the strength did not appreciable vary. In addition, the concrete was cast from the same batch. The yield stresses of the longitudinal and transverse reinforcement were 532 MPa and 332 MPa respectively as obtained from tensile tests on 3 test coupons. Modulus of elasticity and ultimate strain of carbon FRP was determined by coupon tests on 5 times 15 mm wide FRP coupons and was found to be 243 GPa and 1.1% respectively.

Table 2. Tested concrete properties

Connection ID	Cylinder strength MPa	Mod. of elasticity MPa	Tensile strength MPa	Modulus of Rupture MPa
CS1	25.4	24178	2.82	4.38
CF1	25.6	24081	2.51	5.31
CF2	25.6	24242	2.67	4.54

Test Set-up, Instrumentation and Experimental Procedure

The test set-up is shown in Figure 4. The column component of the connection was orientated parallel to the ground while the load was applied to free end of the vertically orientated beam. The connection was mounted on a stiff test rig with hinge supports at both ends of the column. An axial load of 180 kN (equal to 8% of gross axial load capacity of the column and representative of a floor load) was applied to the column using a hydraulic jack attached to one end of the column through a system of high strength bars. A monotonically increasing load was applied to the beam tip through an actuator mounted on a stiff reaction frame. The beam-tip load (herein

referred to as *load*) was applied in increments of 10 kN. At each load increment, the load was paused and cracks were marked on the test specimen. The load was applied using a deflection controlled mode in all tests and the rate of loading used was 0.2 mm per second. At approximately 70% of the theoretical failure load, the load was applied continuously until failure.

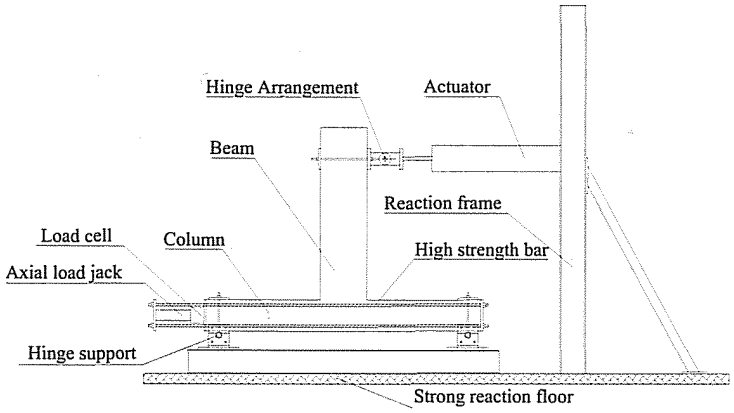

Figure 4. Test setup

Twelve LVDTs were used, three to measure deflection along the length of the beam while the rest were used for monitoring possible movement at key location such as the supports and other critical regions of the test rig. External electric strain gauges on the concrete surface and internal gauges on the steel reinforcing bars were also used for strain measurement. Additional gauges were applied on FRP surfaces for FRP-strengthened connections CF1 and CF2. Seven strain gauges were attached on each FRP strip on the front face and 3 gauges each on the back face for connection CF1 and 9 gauges on each FRP strip (5 on front, 2 on back and 2 on bottom face) for connection CF2 as shown in Figure 3a and 3b respectively. Inclinometers were used to measure rotation at the joint centre and one of the supports. Only a selection of these results will be presented in the following sections.

EXPERIMENTAL RESULTS

Cracking Behaviour and Failure Mode

Control connection CS1

The connection failed by shear failure in the joint. In the early stage of the test, minor flexural cracks were observed in the beam followed by cracks at the beam-column corner. With further increment in the load, severe diagonal shear crack was observed in the joint region at a load of 70 kN (13.2 mm deflection). The peak load of 96.4 kN (27.7 mm) was observed following which the connection lost its load carrying capacity owing to severe shear cracking in the joint region. The test was stopped shortly after the peak load was reached. The final crack pattern is shown in Figure 5a where the average shear crack is orientated at approximately 34 degrees to the horizontal (column) axis.

FRP strengthened connection CF1

Some minor flexural cracks were observed in the beam as it was loaded up to a load of 10 kN. Cracks developed at the beam-column corner at a load of 20 kN (2 mm deflection). Cracks at the beam-column corner propagated towards the joint centre with increasing load until it intersected the FRP then propagated along the direction of FRP. Diagonal crack in the joint region was observed as load was increased from 70 kN to 80 kN (19 mm deflection) and cracking noise was heard indicating localised debonding of FRP at the same time. Last crack marking was carried out at a load of 90 kN following which the specimen was loaded continuously. The peak load of 103 kN was achieved at a deflection of 32 mm when FRP strip 1 (refer to Figure 7a) debonded along its whole length followed by a loss of load carrying capacity of the connection. The connection failed by joint shear failure and concrete spalling was observed at the beam-column corner on the compression face of the beam following the local debonding of FRP strips The column wraps which secured the ends of the FRP strips prevented the strips from complete debonding. The final crack pattern in the joint region is shown in Figure 5b and the average shear crack angle was measured to be at 30 degrees to the column axis. No rupture of the FRP was observed and the FRP provided little restraint to opening of critical shear cracks.

FRP strengthened connection CF2

A fine crack was observed at the beam column corner as the connection was loaded to 10 kN which propagated horizontally towards the beam centre as the load was increased. Further increase of load resulted in the crack to propagate horizontally towards the beam centre and cross the FRP strips, while flexural cracks were observed in the beam. Unlike connection CF1, severe diagonal cracking in the joint region was not observed until the load reached 80 kN (11.5 mm deflection). This was attributed to the confining action provided by the FRP strengthening where the FRP strips around the column and anchored by the FRP wrap restrained the joint against distortion. At 80 kN load (11.5 mm deflection), local debonding of FRP in the FRP strip number 3 (refer to Figure 8a) was observed and the load dropped. The last crack marking was carried out at 90 kN load (14.7 mm deflection) where diagonal shear cracking was observed to form in the joint region, following which the connection was loaded continuously. A peak load of 122 kN was achieved at a deflection of 39.1 mm when FRP strip number 3 (refer to Figure 8a) debonded. This was followed by debonding of FRP strips 2 and 1. The connection lost its load carrying capacity considerably as a result of shear failure which followed debonding along the length of all three FRP strips. Spalling of concrete at the beam-column corner on the compression face was also observed. Sequential rupture of FRP strips 3, 2 and 1 occurred as the loading was continued at load/deflection of 98 kN/67 mm, 81 kN/81.5 mm and 62 kN/92 mm respectively. The final crack pattern is shown in Figure 5c and the average shear crack angle was measured to be at 30 degrees to the column axis.

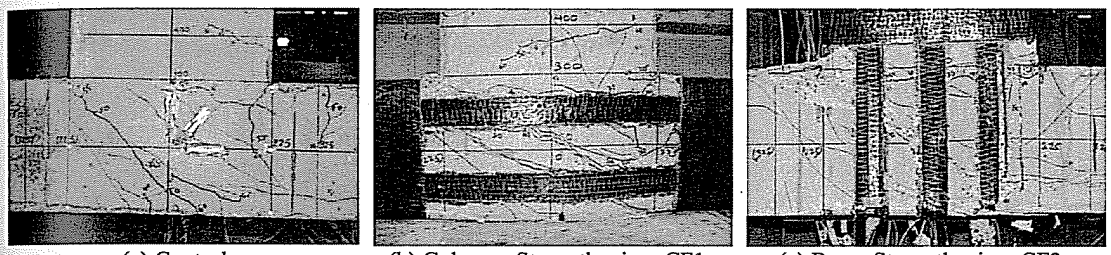

(a) Control (b) Columns Strengthening: CF1 (c) Beam Strengthening: CF2

Figure 5. Final crack patterns for all tested connections.

Load-deflection Response

The load-deflection response for all three connections is shown in Figure 6. Enhancement of the load carrying capacity of the connections due to the FRP is evident in addition to the increase in stiffness. Table 3 is a summary of the peak loads and corresponding deflection for all three connections. FRP strengthening used on connection CF2 was more effective than strengthening on connection CF1. This is not only because the two FRP strengthened connections CF1 and CF2 were designed with different amounts of FRP (but with same FRP area to cross-sectional area ratio) but also because the FRP strengthening in connection CF2 provided confinement in the joint region and restraint against joint rotation. Rupture of FRP on connection CF2, unlike in case of connection CF1, also justifies the effectiveness of the beam strips. The strain distribution on FRP strips, discussed in the next section, also shows that the capacity of beam FRP strips was utilized more effectively than the column FRP strips. The need for corner rounding at the column corners before FRP application to prevent against possible stress concentration and subsequent FRP rupture makes the beam strip arrangement more labour intensive to implement in existing two-dimensional frames compared to the column strip arrangement.

FRP Strain Results

One of the key features of this study was the determination of strain distribution along the length of FRP strips in connections tests CF1 and CF2. The strain distribution for both column oriented strips in connection CF1 are shown in Figure 7 while Figure 8 shows the distribution of strain along the length of the three beam oriented FRP strips for connection CF2. Positions where the shear cracks intersected the FRP strips (indicated by the vertical dashed lines in Figures 7b, 7c, and 8b to 8d) and debonding strains calculated according to the Chen and Teng's (2001) bond strength model (best fit model) (to be discussed in the next section) have also been shown in the strain plots.

Referring to Figure 7, high FRP strain can be observed in the region adjacent to shear cracks indicating debonding of FRP while low FRP strain regions are those where the bond between FRP and concrete was not lost and full shear transfer between the two was maintained. Similar behaviour can be seen in the FRP strain plots of connection CF2 as shown in Figure 8. The reasonably uniform distribution of strain at high load in strip 1 of connection CF1 (Figure 8b and at a limited degree in Figure 8c) indicates the strip has debonded along a

significant portion of its length. Also, even though the final mode of failure in FRP was by rupture in connection CF2, the full rupture strain (1.1% obtained by coupon test) was never attained, primarily due to the bending of FRP strips around the edge of the joint region. Such a phenomenon has been observed in FRP shear-strengthened beams and confined prismatic columns in which the FRP has been wrapped around a bend or corner.

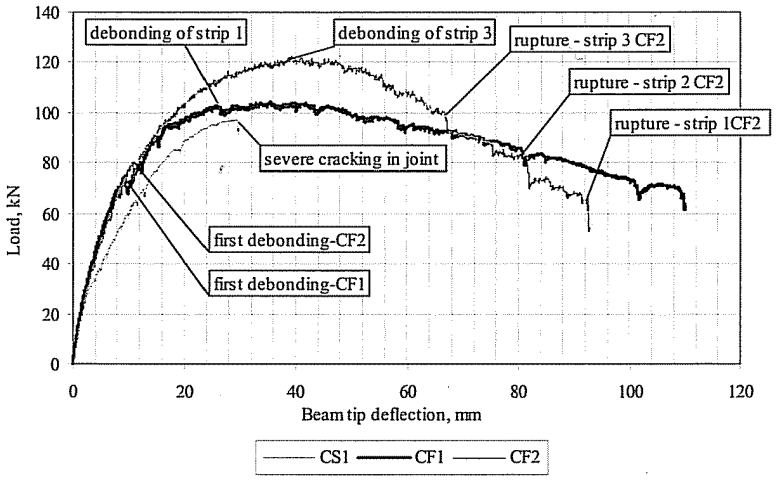

Figure 6. Load versus beam-tip deflection response

Table 3. Summary of load and deflection for all connections

Connection	Peak Load	Deflection	Load increase	Load increase %
CS1	96.4	26.7	-	-
CF1	103	32	6.6	6.8
CF2	122	39.1	25.6	26.5

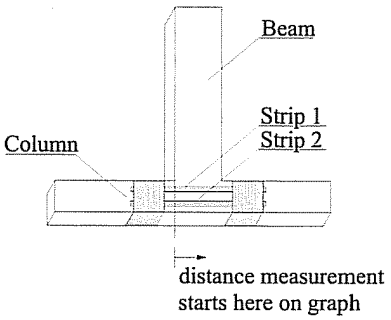

(a) FRP strip labelling

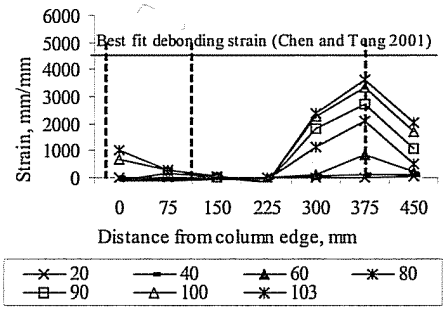

(b) Strip 1

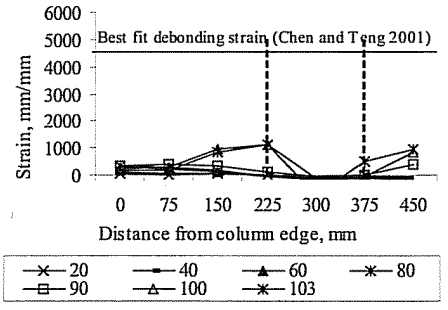

(c) Strip 2

Figure 7. Distribution of strain along length of each FRP strip (dashed lines indicate position where the FRP strips are intersected by shear crack)

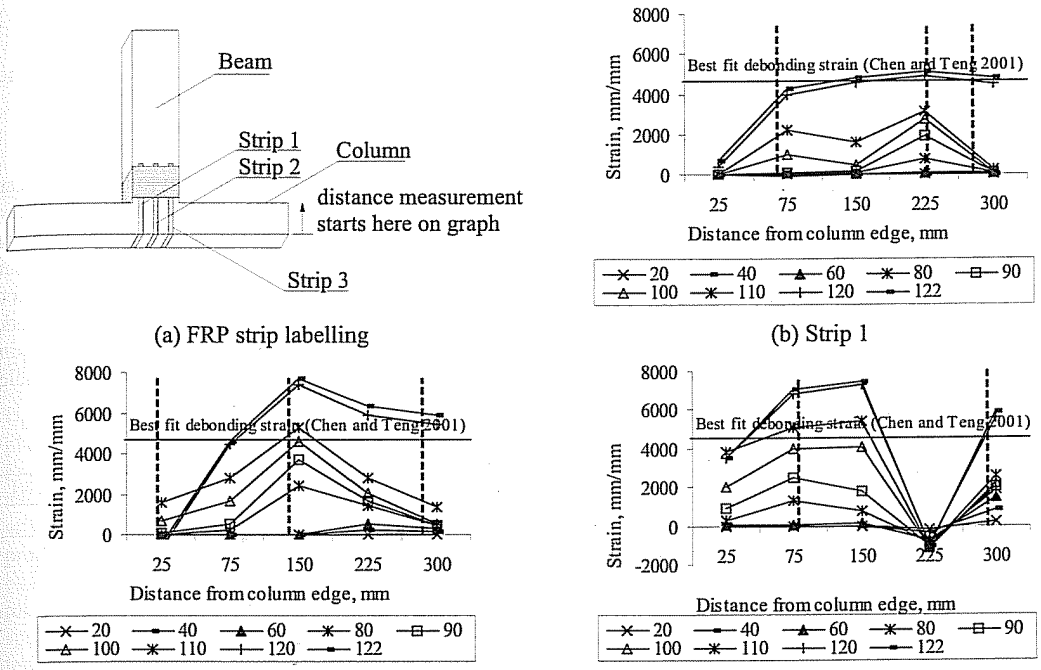

Figure 8. Distribution of strain along length of each FRP strip (dashed lines indicate position where the FRP strips are intersected by shear crack)

ANALYTICAL MODELLING

Strain Estimation

According to the load-deformation plot given in Figure 6, the peak load of the connection was recorded upon debonding of strip 1 for connection CF1 and the debonding of strip 3 for connection CF2; afterwards the load reduced. Debonding is therefore taken as the failure mode for both strengthened. The effectiveness of Chen and Teng's (2001) bond strength model to predict debonding, originally developed from lap-shear tests and later incorporated in Chen and Teng's (2003) model for FRP shear-strengthened beams, is now assessed. Based on this model, the bond strength of FRP bonded to concrete is given by $\sigma_p = \alpha\beta_p\beta_l\sqrt{E_p\sqrt{f'_c}/t_p}$. The parameters α, β_p, β_l, E_p, f'_c *and* t_p represent an empirical factor (best fit model = 0.427), FRP width factor, FRP length factor, modulus of elasticity of FRP and compressive strength of concrete respectively. The FRP width factor is given by $\sqrt{(2-b_p/b_c)/(1+b_p/b_c)}$ where b_p and b_c represent FRP width and concrete width. The FRP length factor is governed by the length of the FRP bonded to concrete and is taken as 1 as the debonded length of FRP at peak load was greater than the effective bond development length (Cao et al. 2005). The input parameters are the same for connections CF1 and CF2, namely, b_p = 50 mm, b_c = 150 mm, E_p = 243,000 MPa, f'_c = 25.6 MPa, and t_p = 0.234 mm, which results in a stress of 1094 MPa. Note that the width of concrete considered effective for each strip is the same for connections CF1 and CF2 (i.e. 2 strips across the 300 mm column width for CF1, and 3 strip down the depth of the 450 mm deep beam for CF2). The strain corresponding to a debonding stress of 1094 MPa is shown in the strain plots of CF1 in Figure 7 and CF2 in Figure 8.

Chen and Teng's (2001) model overestimates the peak strain in strip 1 of CF1 as shown in Figure 2. The model however underestimates the peak strain in strip 3 of CF2 as shown in Figure 8c. The strain in strip 1 in connection CF2, which debonded well after the peak load, correlates very well with the Chen and Teng model prediction as seen in Figure 8b. The accuracy of the model is therefore hypothesised, based on the limited test data, to depend on the debonded length of FRP and the distribution is strain along the length of the FRP.

Contribution of FRP to Shear Strength

The following analytical model, given by Equation (1), is proposed for determining the contribution of FRP to the shear strength of a joint failing by debonding.

$$v_{frp} = \frac{1}{bd}\sum_{i=1}^{n}\left[A_{frp,i}.f_{u,i}\left(Sin\beta.Cos\theta + Sin\theta.Cos\beta\right)\right] \quad (1)$$

where, θ is the angle between critical diagonal crack and column axis, n is the number of layers of FRP, β is the orientation of the FRP layer under consideration to the column axis, b is the joint width, d is the joint depth, $f_{u,i}$ the stress in the FRP at debonding, and $A_{frp,i}$ is the cross-sectional area of FRP strip crossing the joint.

Table 4 shows the values of these parameters considered when calculating the FRP contribution to the joint shear strength for connections CF1 and CF2 and also shows comparison with experimental results. The results show that the proposed model predictions based on strain and crack angle values taken from test results correlates very well with the test data. However, on selecting a general shear crack angle of 45 degrees and using the strain predictions obtained from Chen and Teng's (2001) model, the proposed model over predicts the test result for connection CF1 by 40% while under-predicts the test result for connection CF2 by about 50%. Further work needs to be done to develop this model in particular the development of a strain distribution model. The strain distribution model proposed by Chen and Teng (2003) do does not appreciably help with the predictions of Table 4. It can improve the prediction for CF1[#2] but not for CF2[#2]

Table 4. Summary of input parameters for proposed analytical model

Connection	b mm	d mm	A_{frp} mm^2	f_u MPa	β Deg.	θ Deg.	V_{frp} model MPa	V_{frp} test MPa[#3]	v_{frp} model / v_{frp} test
CF1[#1]	300	300	46.8	876	0	37	0.27	0.28	0.98
CF2[#1]	300	300	70.2	1776	90	30	1.16	1.14	1.02
CF1[#2]	300	300	46.8	1094	0	45	0.40	0.28	1.4
CF2[#2]	300	300	70.2	1092	90	45	0.6	1.14	0.52

[#1] Based on test debonding strain at peak load and observed crack angle
[#2] Based on strain result from Chen and Teng's (2001) model and crack angle of 45°
[#3] Calculated by subtracting the joint shear stress of the control connection CS1 from the FRP-strengthened connection. A detailed description of the calculation of the joint shear stress is given in Shrestha and Smith (2007)

CONCLUSIONS

This paper has demonstrated the effectiveness of FRP in repairing exterior connections using simple and practical strengthening techniques. Beam and/or column wrapping at the ends of the FRP strengthening did not however prove effective in preventing debonding failure of the connections; future strengthening schemes should address this issue. An analytical model to predict the contribution of FRP to the joint shear strength was proposed and outputs compared against test results. The need for inclusion of a suitable FRP strain distribution factor to produce more accurate predictions was identified.

ACKNOWLEDGMENTS

This project was funded by Australian Research Council (ARC) Discovery Grant DP0559567. The financial assistance of the ARC is gratefully acknowledged.

REFERENCES

ACI 440 (2002). *Guide for the Design and Construction of Externally Bonded FRP Systems for Strengthening Concrete Structures*, American Concrete Institute (ACI), Committee 440, Michigan, USA

Cao, S.Y., Chen, J. F., Teng, J. G., Hao, Z. and Chen, J. (2005). "Debonding in RC beams shear strengthened with compete FRP wraps", *Journal of Composites for Construction*, ASCE, 9(5), 417-128.

Chen, J.F. and Teng, J.G. (2001). "Anchorage strength models for FRP and steel plates bonded to concrete", *Journal of Structural Engineering*, ASCE, 125(7), 784-791.

Chen, J.F. and Teng, J.G. (2003). "Shear capacity of FRP-strengthened RC beams: FRP debonding", *Construction and Building Materials*, 17, 27 - 41.

Engindeniz, M., Kahn, L.F. and Zureick, A.H. (2005). "Repair and strengthening of reinforced concrete beam-column joints: state of the art", *ACI Structural Journal*, 102(2), 1-14.

Shrestha, R. and Smith, S.T. (2007). "Behaviour of FRP-strengthened RC beam-column connections", *in preparation*.

Smith, S.T. and Shrestha, R. (2006). "A review of FRP-strengthened RC beam-column connections", *Proceedings, Third FRP Conference on FRP Composites in Civil Engineering*, CICE 2006, Eds. A. Mirmiran and A. Nanni, 13-15 December, Miami, USA.